PERGAMON

International Journal of Heat and Mass Transfer 44 (2001) 3481–3497

International Journal of HEAT and MASS TRANSFER

www.elsevier.com/locate/ijhmt

# Analysis of flow reversal for laminar mixed convection in a vertical rectangular duct with one or more isothermal walls

A. Barletta *

*Dipartimento di Ingegneria Energetica, Nucleare e del Controllo Ambientale (DIENCA), Universitá di Bologna. Viale Risorgimento 2, I-40136 Bologna, Italy*

Received 12 April 2000; received in revised form 11 November 2000

**Abstract**

An investigation of laminar and fully developed mixed convection in a vertical rectangular duct is presented. The analysis refers to thermal boundary conditions such that at least one of the four duct walls is kept isothermal. The evaluation of the velocity field and of the temperature field is performed analytically. The limiting case of free convection, i.e. the case of pure buoyancy-driven flow, is discussed. Special attention is devoted to the following sets of thermal boundary conditions: (A) two facing duct walls are kept isothermal with different temperatures and the others are kept insulated; (B) two facing duct walls have a uniform wall heat flux and the others are kept isothermal with the same temperature. In both cases, the conditions for the onset of flow reversal are obtained. The friction factor is evaluated. It is shown that this parameter depends only on the duct aspect ratio in case (A), while it depends also on the ratio between the Grashof number and the Reynolds number in case (B). 

*Keywords:* Laminar flow; Mixed convection; Rectangular duct; Analytical methods

## 1. Introduction

Several analyses of heat transfer in ducts with non-circular cross section are available in the literature. In most cases, the studies in this field are stimulated by the need for enhancing heat transfer, for instance in the design of compact heat exchangers or of solar collectors. A wide literature refers to the simplest non-circular ducts, i.e., parallel-plate and rectangular ducts. Hartnett and Kostic [1] provide a very deep review of the most important results on heat transfer in rectangular ducts, both for forced and for mixed convection flows. One of the first theoretical analyses of laminar convection in rectangular ducts can be found in Han [2]. In this paper, one can find an analytical solution of momentum and energy balance equations in the case of fully developed mixed convection in a rectangular duct with H1 boundary conditions, namely an axially uniform wall heat flux and a peripherally uniform wall temperature. Iqbal et al. [3] present an analysis of combined forced and free flow in vertical ducts such that the shape of the cross section is a regular polygon. This study includes square ducts and refers to H1 and H2 boundary conditions. The latter boundary condition applies to a duct with both axially and peripherally uniform wall heat flux. A numerical solution for fully developed mixed convection in an inclined rectangular duct is provided for H1 boundary conditions in a paper by Ou et al. [4]. More recently, Aparecido and Cotta [5] develop an investigation of laminar forced convection in the thermal entrance region of a rectangular duct with uniform wall temperature, by employing a generalized integral transform technique. Nonino and Del Giudice [6] provide a numerical study of laminar mixed convection in the entrance region of a horizontal rectangular duct with an arbitrary combination of uniformly heated and adiabatic sides of the rectangle. Gao and Hartnett [7,8] present analyses of fully developed forced convection in a rectangular duct which refer either to laminar flow of a

* Tel.: +39-51-2093-295; fax: +39-51-2093-296.

*E-mail address:* antonio.barletta@mail.ing.unibo.it (A. Barletta).

0017-9310/01/$ - see front matter 
PII: S0017-9310(01)00016-3

**Nomenclature**

| | |
|---|---|
| $a, b$ | length of the rectangle sides |
| $C_1(\sigma), C_2(\sigma)$ | functions defined by Eqs. (29) and (58), respectively |
| $D$ | $2ab/(a+b)$, hydraulic diameter |
| $f$ | Fanning friction factor, defined in Eq. (16) |
| $F(x, y)$ | arbitrary function |
| $g$ | magnitude of the gravitational acceleration |
| $Gr$ | Grashof number, defined in Eq. (8) |
| $(Gr/Re)_{\rm rev}$ | threshold value of $Gr/Re$ for the onset of flow reversal |
| $k$ | thermal conductivity |
| $n, m$ | positive integers |
| $M$ | arbitrary real number employed in Eqs. (24) and (56) |
| $p$ | pressure |
| $P$ | difference between the pressure and the hydrostatic pressure |
| $q_{\rm w}$ | wall heat flux |
| $Re$ | Reynolds number, defined in Eq. (8) |
| $t$ | dimensionless temperature defined in Eq. (8) |
| $T$ | temperature |
| $T_0$ | mean temperature in a duct section |
| $T_1, T_2$ | wall temperatures |
| $u$ | dimensionless velocity defined in Eq. (8) |
| $u^*$ | dimensionless velocity defined in Eq. (31) |
| $\bar{u}^*$ | average value of $u^*(x,y)$ in the region $\{0<x<1, 0<y<\sigma/2\}$ |
| $U$ | $Z$-component of the fluid velocity |
| $U_0$ | mean fluid velocity in a duct section |
| $x, y$ | dimensionless coordinates defined in Eq. (8) |
| $X, Y, Z$ | rectangular coordinates |
| $w$ | arbitrary real variable employed in Eqs. (24) and (25) |
| $\alpha$ | thermal diffusivity |
| $\beta$ | volumetric coefficient of thermal expansion |
| $\Delta T$ | reference temperature difference |
| $\eta$ | dimensionless parameter defined in Eq. (8) |
| $\theta$ | dimensionless temperature, $t-\eta$ |
| $\lambda$ | dimensionless parameter defined in Eq. (8) |
| $\mu$ | dynamic viscosity |
| $\nu$ | kinematic viscosity, $\mu/\rho_0$ |
| $\rho$ | mass density |
| $\rho_0$ | mass density for $T=T_0$ |
| $\sigma$ | aspect ratio defined in Eq. (8) |
| $\tau_{{\rm w},m}$ | average wall shear stress |

*Superscripts*

| | |
|---|---|
| $\sim$ | finite Fourier sine transform defined by Eq. (48) |
| $\approx$ | double finite Fourier sine transform defined by Eq. (18) |

power-law fluid [7] or to slug flow [8]. Both these papers investigate the eight fundamental combinations of uniformly heated and adiabatic sides of the rectangle. By means of an implicit finite difference scheme, Chung et al. [9] investigate thermally-developing forced convection in a rectangular duct with laminar flow and H2 boundary conditions. Spiga and Morini [10] yield an extension of the treatment proposed by Gao and Hartnett [8] in order to determine analytically the developing Nusselt number and the thermal entrance length. By employing the vorticity–velocity formulation, Lee [11] presents a numerical investigation of buoyancy-induced heat and mass transfer in a vertical rectangular duct such that three sides are adiabatic, while the fourth is either isothermal or isoflux. A theoretical investigation of buoyancy induced flow in the fully developed region of a vertical rectangular duct with two isothermal walls and two adiabatic walls has been performed by McBain [12]. In a recent paper [13], the effect of viscous dissipation on slug flow heat transfer in the thermal entrance region of rectangular ducts has been analysed with reference to the eight fundamental H2 boundary conditions considered by Gao and Hartnett [7,8].

As is well known, the parallel-plate channel is a limiting case of a rectangular duct with a very small aspect ratio. Several investigations of the fully developed mixed convection in vertical or inclined parallel-plate channels either with uniform and unequal wall temperatures [14–17] or with uniform wall heat fluxes [15,16] are available in the literature. These theoretical studies are mainly concerned with the modifications of the velocity profiles induced by the buoyancy effect, with a special interest for the conditions which lead to flow reversal. Indeed, flow reversal occurs when the buoyancy force is so strong that there exists a domain within the duct where the fluid velocity has a direction opposite to the mean fluid flow. As a consequence, in the fully developed region, the conditions for flow reversal are determined when one obtains the threshold value of the ratio between the Grashof number $Gr$ and the Reynolds number $Re$ beyond which the phenomenon of flow reversal takes place.

The aim of the present paper is to improve the analyses performed in the case of vertical parallel-plate channels [14–16], by investigating the fully developed mixed convection in vertical rectangular ducts. More precisely, the temperature and velocity fields as well as the friction factor will be evaluated analytically for a given value of $Gr/Re$, with reference to thermal boundary conditions such that at least one of the four sides of the duct is kept isothermal. Then, the conditions for the onset of flow reversal will be determined. Special attention will be devoted to a pair of sample cases: (A) two facing sides are isothermal with different temperatures and the others are insulated; (B) two facing sides have a uniform wall heat flux and the others are isothermal with the same temperature. Finally, the limiting case of pure buoyancy-driven flow, i.e., free convection, will be investigated.

## 2. Governing equations

In this section, the set of balance equations governing the combined forced and free flow in a vertical rectangular duct is written in a dimensionless form.

Let us consider the steady laminar flow of a Newtonian fluid in a vertical rectangular duct with infinite length. Moreover, let us assume that the Boussinesq approximation holds and that the viscous dissipation as well as the temperature changes of the thermal conductivity $k$ and of the dynamic viscosity $\mu$ can be neglected. A drawing of the system examined and of the coordinate axes is reported in Fig. 1. Let us assume that the flow is parallel, i.e. that the only non-vanishing component of the velocity field is the $Z$-component, $U$. Since the Boussinesq approximation implies that the velocity field is solenoidal, it is easily inferred that $U$ cannot depend on $Z$. As a consequence, the momentum balance equations along the directions $X$, $Y$ and $Z$ yield

$$\frac{\partial P}{\partial X}=0, \quad \frac{\partial P}{\partial Y}=0, \tag{1}$$

$$\rho_0 g\beta(T-T_0)-\frac{\partial P}{\partial Z}+\mu\left(\frac{\partial^2 U}{\partial X^2}+\frac{\partial^2 U}{\partial Y^2}\right)=0, \tag{2}$$

where $P=p+\rho_0 gZ$ is the difference between the pressure and the hydrostatic pressure. The reference temperature $T_0$, which appears in Eq. (2), should ensure the best conditions for the validity of the linear relation between the local mass density and the local temperature

$$\rho=\rho_0[1-\beta(T-T_0)]. \tag{3}$$

The usual structure of the Boussinesq approximation can be maintained even if the reference temperature $T_0$ is varying in the streamwise direction. Indeed, in that case, one neglects the change of $\rho_0$ in the streamwise direction. The latter assumption is Morton's hypothesis [18,19] and is widely employed in the literature, whenever the thermal boundary conditions are such that a net heating or cooling of the fluid occurs.

As is discussed in [20], the requirement that $T_0$ must yield the smallest errors in the use of Eq. (3) is fulfilled if the reference temperature $T_0$ coincides with the mean temperature in a duct section, i.e.

$$T_0=\frac{1}{ab}\int_0^a \mathrm{d}X\int_0^b \mathrm{d}Y\, T. \tag{4}$$

Eq. (1) implies that $P$ depends only on $Z$. If Eq. (2) is derived with respect to $Z$, one obtains

$$\frac{\partial T}{\partial Z}=\frac{\mathrm{d}T_0}{\mathrm{d}Z}+\frac{1}{\rho_0 g\beta}\frac{\mathrm{d}^2 P}{\mathrm{d}Z^2}. \tag{5}$$

By employing Eq. (4), Eq. (5) allows one to conclude that $\mathrm{d}P/\mathrm{d}Z$ is a constant and that $\partial T/\partial Z$ coincides with $\mathrm{d}T_0/\mathrm{d}Z$. As a consequence, the energy balance equation can be expressed as

$$U\frac{\mathrm{d}T_0}{\mathrm{d}Z}=\alpha\left(\frac{\partial^2 T}{\partial X^2}+\frac{\partial^2 T}{\partial Y^2}+\frac{\mathrm{d}^2 T_0}{\mathrm{d}Z^2}\right). \tag{6}$$

Moreover, one can easily infer that $\partial T/\partial Z$ depends neither on $X$ nor on $Y$, i.e., the quantity $\partial T/\partial Z$ is uniform in a duct section. Therefore, if at least one of the duct walls is isothermal, then $\partial T/\partial Z$ vanishes identically. In the following, it will be assumed that one or more duct walls are kept isothermal with a temperature $T_1$, so that $\partial T/\partial Z=0$. Under this hypothesis, Eq. (6) can be rewritten as

$$\frac{\partial^2 T}{\partial X^2}+\frac{\partial^2 T}{\partial Y^2}=0. \tag{7}$$

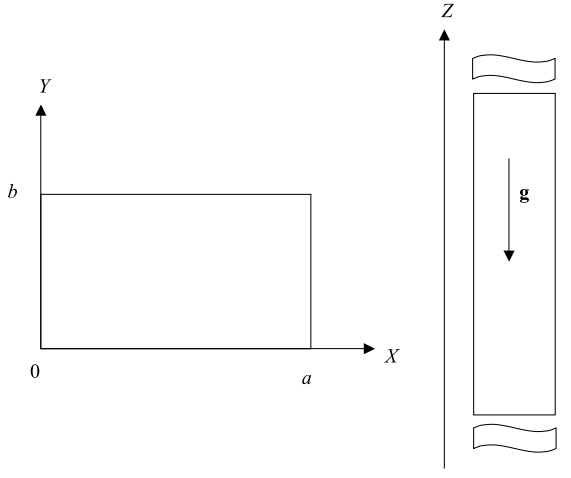


Fig. 1. Drawing of the duct and of the coordinate axes.

The balance equations can be expressed in a dimensionless form by introducing the quantities:

$$t=\frac{T-T_0}{\Delta T},\quad u=\frac{U}{U_0},\quad x=\frac{X}{a},\quad y=\frac{Y}{a},$$
$$\sigma=\frac{b}{a},\quad Re=\frac{U_0 D}{\nu},\quad Gr=\frac{g\beta\Delta T D^3}{\nu^2},$$
$$\eta=\frac{T_1-T_0}{\Delta T},\quad \lambda=-\frac{a^2}{\mu U_0}\frac{\mathrm{d}P}{\mathrm{d}Z}. \tag{8}$$

In Eq. (8), $D=2ab/(a+b)$ is the hydraulic diameter and the mean velocity $U_0$ is defined as

$$U_0=\frac{1}{ab}\int_0^a \mathrm{d}X\int_0^b \mathrm{d}Y\ U, \tag{9}$$

while $\Delta T$ is a reference temperature difference. The latter quantity can be properly fixed once the thermal boundary conditions have been chosen.

On account of Eqs. (2), (7) and (8), the momentum balance equation and the energy balance equation can be expressed as

$$\frac{\partial^2 u}{\partial x^2}+\frac{\partial^2 u}{\partial y^2}=-\frac{(1+\sigma)^2}{4\sigma^2}\frac{Gr}{Re}t-\lambda, \tag{10}$$

$$\frac{\partial^2 t}{\partial x^2}+\frac{\partial^2 t}{\partial y^2}=0. \tag{11}$$

Additional constraints fulfilled by the functions $t(x,y)$ and $u(x,y)$ are provided by Eqs. (4) and (9), namely

$$\int_0^1 \mathrm{d}x\int_0^\sigma \mathrm{d}y\ t=0, \tag{12}$$

$$\int_0^1 \mathrm{d}x\int_0^\sigma \mathrm{d}y\ u=\sigma. \tag{13}$$

The velocity field fulfils no-slip boundary conditions at the duct walls. As a consequence, the boundary conditions satisfied by the dimensionless velocity field can be expressed as

$$u(x,0)=u(x,\sigma)=u(0,y)=u(1,y)=0. \tag{14}$$

The average wall shear stress with respect to the perimeter of the duct is defined as

$$\tau_{w,m}=\frac{\mu}{2(a+b)}\left[\int_0^b \left.\frac{\partial U}{\partial X}\right|_{X=0}\mathrm{d}Y-\int_0^b \left.\frac{\partial U}{\partial X}\right|_{X=a}\mathrm{d}Y+\int_0^a \left.\frac{\partial U}{\partial Y}\right|_{Y=0}\mathrm{d}X-\int_0^a \left.\frac{\partial U}{\partial Y}\right|_{Y=b}\mathrm{d}X\right]. \tag{15}$$

On account of Eq. (15), the Fanning friction factor is given by

$$f=\frac{2\tau_{w,m}}{\rho_0 U_0^2}=\frac{1}{Re}\frac{2\sigma}{(1+\sigma)^2}\left[\int_0^\sigma \left.\frac{\partial u}{\partial x}\right|_{x=0}\mathrm{d}y-\int_0^\sigma \left.\frac{\partial u}{\partial x}\right|_{x=1}\mathrm{d}y+\int_0^1 \left.\frac{\partial u}{\partial y}\right|_{y=0}\mathrm{d}x-\int_0^1 \left.\frac{\partial u}{\partial y}\right|_{y=\sigma}\mathrm{d}x\right]. \tag{16}$$

If one performs a double integration of both sides of Eq. (10) with respect to $x$ in the interval $0\leqslant x\leqslant 1$ and with respect to $y$ in the interval $0\leqslant y\leqslant\sigma$, by employing Eqs. (12) and (16), one obtains the following relation between the parameters $f$ and $\lambda$

$$fRe=\frac{2\sigma^2}{(1+\sigma)^2}\lambda. \tag{17}$$

The solution of Eqs. (10)–(14) together with a suitable set of thermal boundary conditions yields the functions $u(x,y)$ and $t(x,y)$ as well as the parameters $\lambda$ and $\eta$. More precisely, Eqs. (10)–(14) show that one can first determine $t(x,y)$ by solving Eq. (11) with given thermal boundary conditions. Then, Eq. (12) can be employed to obtain $\eta$. By substituting $t(x,y)$ in Eq. (10) and by utilizing the boundary conditions expressed by Eq. (14), one determines the function $u(x,y)$. Finally, the constraint given by Eq. (13) allows one to find out the parameter $\lambda$.

It should be pointed out that, for every choice of the thermal boundary conditions, Eqs. (11) and (12) ensure that the dimensionless temperature field $t(x,y)$ is independent of the dimensionless velocity field $u(x,y)$. In particular, the evaluation of $t(x,y)$ can be performed through the solution of a stationary and two-dimensional heat conduction problem.

## 3. Evaluation of the velocity field

In this section, the dimensionless velocity field $u(x,y)$ is evaluated under the assumption that the dimensionless temperature field $t(x,y)$ has been previously obtained.

Let us assume that the first steps of the solution procedure of Eqs. (10)–(14) have been performed, so that $t(x,y)$ and $\eta$ have been determined. Then, the dimensionless velocity field $u(x,y)$ can be obtained by employing the finite Fourier transforms method. In particular, the double finite Fourier sine transform of an arbitrary function $F(x,y)$ in the domain $0\leqslant x\leqslant 1$, $0\leqslant y\leqslant\sigma$ is defined as [21]

$$\tilde{\tilde{F}}(n,m)=\int_0^1 \mathrm{d}x\int_0^\sigma \mathrm{d}y\ F(x,y)\sin(n\pi x)\sin\left(\frac{m\pi y}{\sigma}\right), \tag{18}$$

where $n$ and $m$ are positive integers. On account of the properties of the finite Fourier transforms widely discussed in [21] and of the boundary conditions given by

Eq. (14), Eq. (10) can be rewritten as an algebraic equation, namely

$$\pi^2\left(n^2+\frac{m^2}{\sigma^2}\right)\tilde{\tilde{u}}=\frac{(1+\sigma)^2}{4\sigma^2}\frac{Gr}{Re}\tilde{\tilde{t}} + \lambda\frac{\sigma}{nm\pi^2}[1-(-1)^n][1-(-1)^m]. \tag{19}$$

Eq. (19) allows the evaluation of $\tilde{\tilde{u}}(n,m)$, one obtains

$$\tilde{\tilde{u}}(n,m)=\frac{\lambda\sigma^3[1-(-1)^n][1-(-1)^m]}{nm\pi^4(\sigma^2n^2+m^2)} + \frac{Gr}{Re}\frac{(1+\sigma)^2\tilde{\tilde{t}}(n,m)}{4\pi^2(\sigma^2n^2+m^2)}. \tag{20}$$

Once the transform $\tilde{\tilde{u}}(n,m)$ has been determined, the dimensionless velocity $u(x,y)$ can be evaluated by employing the inversion formula [21]

$$F(x,y)=\frac{4}{\sigma}\sum_{m=1}^{\infty}\sum_{n=1}^{\infty}\tilde{\tilde{F}}(n,m)\sin(n\pi x)\sin\left(\frac{m\pi y}{\sigma}\right). \tag{21}$$

By substituting Eq. (20) in Eq. (21), one is led to the expression

$$u(x,y)=\frac{16\sigma^2\lambda}{\pi^4} \times\sum_{m=1}^{\infty}\sum_{n=1}^{\infty}\frac{\sin[(2n-1)\pi x]}{(2n-1)(2m-1)[\sigma^2(2n-1)^2+(2m-1)^2]} \times\sin\left[\frac{(2m-1)\pi y}{\sigma}\right]+\frac{(1+\sigma)^2}{\pi^2\sigma} \times\frac{Gr}{Re}\sum_{m=1}^{\infty}\sum_{n=1}^{\infty}\frac{\tilde{\tilde{t}}(n,m)}{\sigma^2n^2+m^2}\sin(n\pi x)\sin\left(\frac{m\pi y}{\sigma}\right). \tag{22}$$

In the limit $Gr/Re\to 0$, the velocity $u(x,y)$ tends to coincide with the first term on the right-hand side of Eq. (22), namely

$$u(x,y)|_{(Gr/Re)\to 0}=\frac{16\sigma^2\lambda}{\pi^4} \times\sum_{m=1}^{\infty}\sum_{n=1}^{\infty}\frac{\sin[(2n-1)\pi x]}{(2n-1)(2m-1)[\sigma^2(2n-1)^2+(2m-1)^2]} \times\sin\left[\frac{(2m-1)\pi y}{\sigma}\right]. \tag{23}$$

The dimensionless velocity distribution expressed by Eq. (23) occurs in the absence of buoyancy forces, i.e., in the case of forced convection. The expression of the dimensionless velocity field given by Eq. (23) is equal to the one obtained in the case of isothermal flow by Spiga and Morini [22]. On the other hand, by employing Fourier series expansions in the interval $0\leqslant w\leqslant 1$, the following mathematical identities are easily proved:

$$\frac{\pi}{4M^2}\left\{1-\frac{\cosh[M\pi(w-1/2)]}{\cosh[M\pi/2]}\right\} =\sum_{n=1}^{\infty}\frac{\sin[(2n-1)\pi w]}{(2n-1)[M^2+(2n-1)^2]}, \tag{24}$$

$$\frac{\pi^3}{8}w(1-w)=\sum_{n=1}^{\infty}\frac{\sin[(2n-1)\pi w]}{(2n-1)^3}. \tag{25}$$

As a consequence of Eqs. (24) and (25), the double infinite sum on the right-hand side of Eq. (23) can be written as a single infinite sum either as

$$u(x,y)|_{(Gr/Re)\to 0}=\frac{4\lambda}{\pi^3}\sum_{n=1}^{\infty} \times\left\{1-\frac{\cosh[(2n-1)\pi(y-\sigma/2)]}{\cosh[(2n-1)\pi\sigma/2]}\right\} \times\frac{\sin[(2n-1)\pi x]}{(2n-1)^3}=\frac{\lambda}{2}x(1-x) -\frac{4\lambda}{\pi^3}\sum_{n=1}^{\infty}\frac{\cosh[(2n-1)\pi(y-\sigma/2)]}{(2n-1)^3\cosh[(2n-1)\pi\sigma/2]} \times\sin[(2n-1)\pi x], \tag{26a}$$

or as

$$u(x,y)|_{(Gr/Re)\to 0}=\frac{4\sigma^2\lambda}{\pi^3}\sum_{n=1}^{\infty}\frac{1}{(2n-1)^3} \times\left\{1-\frac{\cosh[(x-1/2)(2n-1)\pi/\sigma]}{\cosh[(2n-1)\pi/(2\sigma)]}\right\} \times\sin\left[\frac{(2n-1)\pi y}{\sigma}\right]=\frac{\lambda}{2}y(\sigma-y) \times-\frac{4\sigma^2\lambda}{\pi^3}\sum_{n=1}^{\infty}\frac{\cosh[(x-1/2)(2n-1)\pi/\sigma]}{(2n-1)^3\cosh[(2n-1)\pi/(2\sigma)]} \times\sin\left[\frac{(2n-1)\pi y}{\sigma}\right]. \tag{26b}$$

The expression which appears in Eq. (26a) agrees with the classical mathematical form of the dimensionless velocity for fully developed isothermal flow in a rectangular duct available, for instance, in [23]. Although Spiga and Morini [22] emphasize the very fast convergence of the double series expression given by Eq. (23), it is quite obvious that both the single series expression which appears in Eq. (26a) and that which appears in Eq. (26b) converge faster and, as a consequence, are preferable.

In [22], a table with values in the limit $Gr/Re\to 0$ of the ratio $u(x,y)/\lambda$ at different positions in the duct cross-section is reported for $\sigma=1$. A comparison between these values and those evaluated by employing Eq. (26a) is performed in Table 1. This table shows that the relative discrepancy ranges from 0.29% to 0.64%. Since analytical solutions are involved, these relative discrepancies are not so small. This circumstance is somewhat

Table 1
Values of $u(x,y)/\lambda$ for $Gr/Re \to 0$ and $\sigma = 1$

| $(x,y)$ | $u(x,y)/\lambda$ evaluated by Eq. (26a) | $u(x,y)/\lambda$ Ref. [22] |
|---|---|---|
| (0.5, 0.5) | 0.07367135 | – |
| (0.5, 0.75) (0.75, 0.5) | 0.05733491 | 0.05750080 |
| (0.6, 0.6) | 0.06874431 | – |
| (0.6, 0.75) (0.75, 0.6) | 0.05549793 | 0.05566930 |
| (0.75, 0.75) | 0.04528616 | – |
| (0.85, 0.75) (0.75, 0.85) | 0.03236660 | 0.03252332 |
| (0.85, 0.85) | 0.02360474 | – |
| (0.9, 0.75) (0.75, 0.9) | 0.02356374 | 0.02371376 |
| (0.9, 0.9) | 0.01307145 | – |

unexpected, since we have just shown that the expression of the dimensionless velocity distribution found by Spiga and Morini [22] is mathematically coincident with the right-hand side of Eq. (26a). Probably, Spiga and Morini [22] have employed a truncated double-series expression of the velocity field with an insufficient number of terms to ensure a satisfactory convergence.

On account of Eqs. (26b), Eq. (22) can be rewritten as

$$u(x,y) = \frac{\lambda}{2} y(\sigma - y) - \frac{4\sigma^2\lambda}{\pi^3} \sum_{n=1}^{\infty} \frac{\cosh[(x-1/2)(2n-1)\pi/\sigma]}{(2n-1)^3 \cosh[(2n-1)\pi/(2\sigma)]} \times \sin\left[\frac{(2n-1)\pi y}{\sigma}\right] + \frac{(1+\sigma)^2}{\pi^2\sigma} \times \frac{Gr}{Re} \sum_{m=1}^{\infty}\sum_{n=1}^{\infty} \frac{\tilde{\tilde{t}}(n,m)}{\sigma^2 n^2 + m^2} \sin(n\pi x) \sin\left(\frac{m\pi y}{\sigma}\right). \tag{27}$$

The parameter $\lambda$ can be easily evaluated by substituting Eq. (27) into Eq. (13). Then, on account of Eq. (17), one obtains the following expression of the friction factor $fRe$:

$$fRe = \frac{24}{(1+\sigma)^2} \times \frac{1 - \frac{4(1+\sigma)^2}{\pi^4\sigma} \frac{Gr}{Re} \sum_{m=1}^{\infty} \sum_{n=1}^{\infty} \frac{\tilde{\tilde{t}}(2n-1,2m-1)}{(2n-1)(2m-1)[\sigma^2(2n-1)^2+(2m-1)^2]}}{1 - \frac{192\sigma}{\pi^5} \sum_{n=1}^{\infty} \frac{\tanh[(2n-1)\pi/(2\sigma)]}{(2n-1)^5}}. \tag{28}$$

By employing the definition of double finite Fourier sine transform expressed by Eq. (18), the following statement is easily proved. If the thermal boundary conditions lead to a dimensionless temperature distribution $t(x,y)$ which is either antisymmetric with respect to the midplane $x = 1/2$ or antisymmetric with respect to the midplane $y = \sigma/2$, then $\tilde{\tilde{t}}(2n-1, 2m-1) = 0$ for every pair of positive integers $(n,m)$. Obviously, on account of Eq. (28), the latter condition implies that the friction factor is not affected by buoyancy, i.e., that $fRe$ does not depend on $Gr/Re$.

As a consequence of Eq. (28), in the special case of isothermal flow, i.e., in the limit $Gr/Re \to 0$, the friction factor is given by

$$fRe|_{(Gr/Re)\to 0} = \frac{24}{(1+\sigma)^2} \times \left\{1 - \frac{192\sigma}{\pi^5} \sum_{n=1}^{\infty} \frac{\tanh[(2n-1)\pi/(2\sigma)]}{(2n-1)^5}\right\}^{-1} \equiv C_1(\sigma). \tag{29}$$

It can be easily shown that, in the limit $\sigma \to 0$, the right-hand side of Eq. (29) tends to 24. Indeed, in this limit, one recovers the well-known value of $fRe$ for isothermal flow in a parallel-plate channel. Moreover, it is easily verified that function $C_1(\sigma)$ defined by Eq. (29) is such that $C_1(\sigma) = C_1(1/\sigma)$, for every $\sigma$. This conclusion is expected, since $C_1(\sigma)$ yields the value of $fRe$ for isothermal fluid flow, and this quantity depends only on the shape of the duct. Obviously, two rectangular ducts with aspect ratios $\sigma$ and $1/\sigma$, respectively, have the same shape. Values of $C_1(\sigma)$ are reported in Table 2. These values support a fair agreement with the values of $fRe$ for the case $Gr/Re \to 0$ provided in [23].

A special case is obtained when $dP/dZ \to 0$. In this case, Eq. (2) shows that the flow is driven only by the buoyancy force and by the viscous force, i.e., free convection occurs. On account of Eqs. (8) and (17), the above limit implies that both $\lambda \to 0$ and $f \to 0$. Strictly speaking, this conclusion is legitimate only if, in the limit $dP/dZ \to 0$, the mean velocity $U_0$ does not vanish. Otherwise, both $\lambda$ and $f$ would be ill-defined. Therefore, if $U_0$ is nonzero in the limit of free convection, its value can be determined by employing Eq. (28), namely through the condition

$$\left.\frac{Gr}{Re}\right|_{dP/dZ\to 0} = \frac{\pi^4\sigma}{4(1+\sigma)^2} \times \left\{\sum_{m=1}^{\infty}\sum_{n=1}^{\infty} \frac{\tilde{\tilde{t}}(2n-1,2m-1)}{(2n-1)(2m-1)[\sigma^2(2n-1)^2+(2m-1)^2]}\right\}^{-1}. \tag{30}$$

Since Eq. (8) yields $Gr/Re = g\beta\Delta T D^2/(\nu U_0)$, Eq. (30) allows one to evaluate the residual mean fluid velocity $U_0$ in the limit $dP/dZ \to 0$. Eq. (30) is obviously meaningless when the double series on the right-hand side is zero. Indeed, if the thermal boundary conditions are such that the double series on the right-hand side of Eq. (30) vanishes, then the mean velocity $U_0$ tends to zero in the limit $dP/dZ \to 0$. As it has been pointed out above, this circumstance occurs if $t(x,y)$ is either antisymmetric with respect to the midplane $x = 1/2$ or antisymmetric with respect to the midplane $y = \sigma/2$.

Table 2
Values of $C_1(\sigma)$, $C_2(\sigma)$ and $-C_1(\sigma)/C_2(\sigma)$

| $\sigma$ | $C_1(\sigma)$ | $C_2(\sigma)\times 100$ | $-C_1(\sigma)/C_2(\sigma)$ |
|---|---|---|---|
| 0 | 24 | $-\infty$ | 0 |
| 0.01 | 23.6763 | −5.16875 | 458.067 |
| 0.05 | 22.4770 | −4.84033 | 464.369 |
| 0.1 | 21.1689 | −4.44158 | 476.607 |
| 0.2 | 19.0705 | −3.68865 | 517.005 |
| 0.3 | 17.5121 | −3.00627 | 582.518 |
| 0.4 | 16.3681 | −2.40639 | 680.192 |
| 0.5 | 15.5481 | −1.89191 | 821.818 |
| 0.6 | 14.9800 | −1.45640 | 1028.56 |
| 0.7 | 14.6054 | −1.08949 | 1340.57 |
| 0.8 | 14.3778 | −0.780656 | 1841.76 |
| 0.9 | 14.2610 | −0.520724 | 2738.68 |
| 1.0 | 14.2271 | −0.302051 | 4710.16 |
| 1.25 | 14.3778 | 0.102837 | −13981.1 |
| 1.5 | 14.7118 | 0.359586 | −4091.32 |
| 1.75 | 15.1202 | 0.516842 | −2925.50 |
| 2 | 15.5481 | 0.607983 | −2557.32 |
| 2.25 | 15.9683 | 0.655921 | −2434.48 |
| 2.5 | 16.3681 | 0.676156 | −2420.76 |
| 2.75 | 16.7424 | 0.678985 | −2465.79 |
| 3 | 17.0897 | 0.671146 | −2546.34 |
| 3.5 | 17.7069 | 0.639296 | −2769.75 |
| 4 | 18.2328 | 0.599676 | −3040.44 |
| 4.5 | 18.6827 | 0.559806 | −3337.36 |
| 5 | 19.0705 | 0.522442 | −3650.26 |
| 10 | 21.1689 | 0.299701 | −7063.33 |
| 20 | 22.4770 | 0.158532 | −14178.2 |
| 100 | 23.6763 | 0.033016 | −71711.2 |
| $\infty$ | 24 | 0 | $-\infty$ |

Let us define

$$u^* = \frac{Re}{Gr}u = \frac{vU}{g\beta\Delta T D^2}. \tag{31}$$

Then, in the limit $dP/dZ \to 0$, Eq. (27) yields

$$u^*(x,y) = \frac{(1+\sigma)^2}{\pi^2\sigma}\sum_{m=1}^{\infty}\sum_{n=1}^{\infty}\frac{\tilde{\tilde{t}}(n,m)}{\sigma^2 n^2 + m^2} \times \sin(n\pi x)\sin\left(\frac{m\pi y}{\sigma}\right). \tag{32}$$

In the following, Eqs. (27) and (28) will be employed to investigate two special sets of thermal boundary conditions. The set (A) is defined by the conditions

$$\left.\frac{\partial T}{\partial X}\right|_{X=0} = 0, \quad T(X,0,Z) = T_1, \qquad \left.\frac{\partial T}{\partial X}\right|_{X=a} = 0, \quad T(X,b,Z) = T_2, \tag{33}$$

while the set (B) is as follows:

$$k\left.\frac{\partial T}{\partial Y}\right|_{Y=0} = -q_w, \quad T(0,Y,Z) = T_1, \qquad k\left.\frac{\partial T}{\partial Y}\right|_{Y=b} = q_w, \quad T(a,Y,Z) = T_1. \tag{34}$$

A schematic representation of these sets of thermal boundary conditions is reported in Fig. 2.

## 4. Case (A): two isothermal and two adiabatic walls

In this section, the dimensionless temperature field $t(x,y)$ for the set (A) of thermal boundary conditions is evaluated. Then, the dimensionless velocity field and the friction factor are obtained through Eqs. (27) and (28).

A convenient choice of the reference temperature difference is, in this case, $\Delta T = T_1 - T_2$. In this section, it will be assumed that $T_1 > T_2$, so that $\Delta T > 0$. Moreover, this assumption implies that $Gr/Re > 0$ corresponds to upward mean flow ($U_0 > 0$), while $Gr/Re < 0$ corresponds to downward mean flow ($U_0 < 0$). On account of Eqs. (8) and (33), the thermal boundary conditions are expressed in the following dimensionless form:

$$\left.\frac{\partial t}{\partial x}\right|_{x=0} = 0, \quad t(x,0) = \eta, \qquad \left.\frac{\partial t}{\partial x}\right|_{x=1} = 0, \quad t(x,\sigma) = \eta - 1. \tag{35}$$

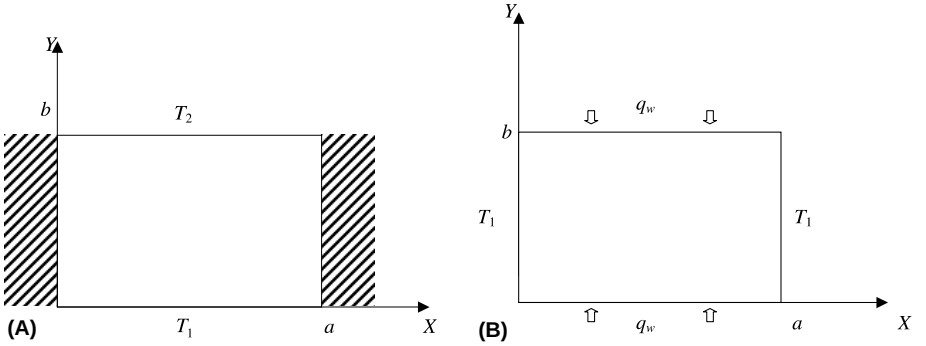


Fig. 2. Thermal boundary conditions.

It can be easily verified that the solution of Eq. (11) with the boundary condition expressed by Eq. (33) is a one-dimensional solution which can be written as

$$t(x,y)=\eta-\frac{y}{\sigma}. \tag{36}$$

Substitution of Eq. (36) in Eq. (12) allows one to obtain $\eta=1/2$. As a consequence of Eq. (18) and of Eq. (36), one is led to the expression

$$\tilde{\tilde{t}}(n,m)=\frac{\sigma}{2nm\pi^2}[1-(-1)^n][1+(-1)^m]. \tag{37}$$

Eqs. (28) and (37) allow one to conclude that the friction factor is not influenced by the buoyancy effect, since Eq. (37) yields $\tilde{\tilde{t}}(2n-1,2m-1)=0$. Indeed, Eq. (36) with $\eta=1/2$ implies that $t(x,y)$ is antisymmetric with respect to the midplane $y=\sigma/2$. Therefore, one obtains

$$fRe=C_1(\sigma), \tag{38}$$

and, on account of Eqs. (17) and (29),

$$\lambda=\frac{12}{\sigma^2}\left\{1-\frac{192\sigma}{\pi^5}\sum_{n=1}^{\infty}\frac{\tanh[(2n-1)\pi/(2\sigma)]}{(2n-1)^5}\right\}^{-1}. \tag{39}$$

Moreover, one can conclude that the set (A) of thermal boundary conditions is such that the mean velocity $U_0$ tends to 0 in the limit $\mathrm{d}P/\mathrm{d}Z\to 0$. Eqs. (27) and (37) yield

$$\begin{aligned}u(x,y)=&\frac{\lambda}{2}y(\sigma-y)\\&-\frac{4\sigma^2\lambda}{\pi^3}\sum_{n=1}^{\infty}\frac{\cosh[(x-1/2)(2n-1)\pi/\sigma]}{(2n-1)^3\cosh[(2n-1)\pi/(2\sigma)]}\\&\times\sin\left[\frac{(2n-1)\pi y}{\sigma}\right]+\frac{(1+\sigma)^2}{\pi^4}\\&\times\frac{Gr}{Re}\sum_{m=1}^{\infty}\sum_{n=1}^{\infty}\frac{\sin[(2n-1)\pi x]}{(2n-1)m[\sigma^2(2n-1)^2+4m^2]}\\&\times\sin\left(\frac{2m\pi y}{\sigma}\right).\end{aligned} \tag{40}$$

On account of Eq. (24), Eq. (40) can be rewritten as

$$\begin{aligned}u(x,y)=&\frac{\lambda}{2}y(\sigma-y)\\&-\frac{4\sigma^2\lambda}{\pi^3}\sum_{n=1}^{\infty}\frac{\cosh[(x-1/2)(2n-1)\pi/\sigma]}{(2n-1)^3\cosh[(2n-1)\pi/(2\sigma)]}\\&\times\sin\left[\frac{(2n-1)\pi y}{\sigma}\right]+\frac{(1+\sigma)^2}{16\pi^3}\frac{Gr}{Re}\sum_{n=1}^{\infty}\frac{1}{n^3}\\&\times\left\{1-\frac{\cosh[(2x-1)n\pi/\sigma]}{\cosh(n\pi/\sigma)}\right\}\sin\left(\frac{2n\pi y}{\sigma}\right)\\=&\left[\lambda+\frac{(1+\sigma)^2}{24\sigma^3}\frac{Gr}{Re}(\sigma-2y)\right]\frac{y(\sigma-y)}{2}\\&-\frac{4\sigma^2\lambda}{\pi^3}\sum_{n=1}^{\infty}\frac{\cosh[(x-1/2)(2n-1)\pi/\sigma]}{(2n-1)^3\cosh[(2n-1)\pi/(2\sigma)]}\\&\times\sin\left[\frac{(2n-1)\pi y}{\sigma}\right]-\frac{(1+\sigma)^2}{16\pi^3}\\&\times\frac{Gr}{Re}\sum_{n=1}^{\infty}\frac{\cosh[(2x-1)n\pi/\sigma]}{n^3\cosh(n\pi/\sigma)}\sin\left(\frac{2n\pi y}{\sigma}\right),\end{aligned} \tag{41}$$

where the Fourier series expansion

$$\frac{\pi^3}{3\sigma^3}y(\sigma-y)(\sigma-2y)=\sum_{n=1}^{\infty}\frac{1}{n^3}\sin\left(\frac{2n\pi y}{\sigma}\right), \tag{42}$$

in the interval $0\leqslant y\leqslant\sigma$, has been employed. As is easily verified, in the limit $a\to\infty$ and $\sigma\to 0$, the expression of $u(x,y)$ given by Eq. (41) is considerably simplified. More precisely, in this limit, the terms containing the infinite sums tend to zero while the first term yields a non-vanishing contribution. By employing Eqs. (8), (39) and (41), one obtains

$$u(x,y)\,|_{\substack{a\to\infty\\ \sigma\to 0}}=\left[6+\frac{1}{48}\frac{Gr}{Re}\left(1-2\frac{Y}{b}\right)\right]\frac{Y}{b}\left(1-\frac{Y}{b}\right). \tag{43}$$

Indeed, the right-hand side of Eq. (43) coincides with the well-known velocity profile for laminar and fully developed flow in a vertical parallel-plate channel with uniform and unequal wall temperatures [14,17].

As is shown in [14,17], Eq. (43) implies that, in a parallel-plate vertical channel, flow reversal next to the cool wall ($Y=b$) occurs if $Gr/Re>288$. On the other hand, at the hot wall ($Y=0$), the flow reversal condition is fulfilled when $Gr/Re<-288$. Indeed, the one-dimensional velocity profile expressed through Eq. (43) is left invariant by the combined transformation $Y\to b-Y$, $Gr/Re\to -Gr/Re$. As a consequence of this symmetry, one can investigate the condition of flow reversal at the cool wall for upward mean flow and then extend easily the result to flow reversal at the hot wall for downward mean flow. The velocity distribution for a rectangular duct expressed by Eq. (41) is symmetric under the transformation $x\to 1-x$. Moreover, this velocity distribution is left invariant by the combined transformation $y\to\sigma-y$, $Gr/Re\to -Gr/Re$. Therefore, one can restrict the investigation to the onset of flow reversal next to the cool wall ($y=\sigma$) with reference to upward mean flow. In this case, an analysis of the velocity profiles given by Eq. (41) allows one to infer that the onset of flow reversal occurs next to the corners ($x=0$, $y=\sigma$) and ($x=1$, $y=\sigma$). Indeed, on account of Eq. (41), one can prove that the derivative $\partial u/\partial y$ vanishes at the point ($x=0$, $y=\sigma$). Moreover, the derivative $\partial^2 u/\partial x\partial y$ at $y=\sigma$ tends to $+\infty$ for $x\to 0$ if $Gr/Re>8\lambda\sigma^2/(1+\sigma)^2$, while it tends to $-\infty$ for $x\to 0$ if $Gr/Re<8\lambda\sigma^2/(1+\sigma)^2$. Therefore, on account of Eqs. (17) and (29), one can conclude that the threshold value

of $Gr/Re$ above which flow reversal occurs next to the corners ($x = 0$, $y = \sigma$) and ($x = 1$, $y = \sigma$) is

$$\left(\frac{Gr}{Re}\right)_{\rm rev} = \frac{8\lambda\sigma^2}{(1+\sigma)^2} = 4C_1(\sigma). \tag{44}$$

The values of $C_1(\sigma)$ reported in Table 2 allow one to evaluate the threshold value $(Gr/Re)_{\rm rev}$ for a given aspect ratio $\sigma$.

On account of Eqs. (31) and (41), in the limit $dP/dZ \to 0$, one obtains the following expression of $u^*(x,y)$:

$$u^*(x,y) = \frac{(1+\sigma)^2}{48\sigma^3}y(\sigma-y)(\sigma-2y) - \frac{(1+\sigma)^2}{16\pi^3} \times \sum_{n=1}^{\infty}\frac{\cosh[(2x-1)n\pi/\sigma]}{n^3\cosh(n\pi/\sigma)}\sin\left(\frac{2n\pi y}{\sigma}\right). \tag{45}$$

It is easily verified that the distribution $u^*(x,y)$ is symmetric with respect to the line $x = 1/2$ and antisymmetric with respect to the line $y = \sigma/2$. More precisely $u^*(x,y)$ is positive in the region $\{0 < x < 1, 0 < y < \sigma/2\}$, while it is negative in the region $\{0 < x < 1, \sigma/2 < y < \sigma\}$. The right-hand side of Eq. (45) agrees with the expression, found by McBain [12], for the fully developed velocity profile of free convection in a vertical rectangular duct with two adiabatic walls and two facing isothermal walls with different temperatures.

By employing Eqs. (29) and (45), one can easily show that the average value of $u^*(x,y)$ in the region $\{0 < x < 1, 0 < y < \sigma/2\}$ is given by

$$\bar{u}^* = \frac{(1+\sigma)^2}{8(2+\sigma)^2 C_1(\sigma/2)}. \tag{46}$$

On account of Eq. (46), one can easily evaluate $\bar{u}^*$ by employing the values of $C_1(\sigma)$ reported in Table 1. One can easily show that $\bar{u}^*$ is a rapidly increasing function of $\sigma$ for $\sigma < 5.0449$, reaches a maximum for $\sigma = 5.0449$ and, for higher aspect ratios, undergoes a slow decrease. The maximum value of $\bar{u}^*$ is $5.6107 \times 10^{-3}$. It is easily verified that $\bar{u}^* \to 1/768$ for $\sigma \to 0$, while $\bar{u}^* \to 1/192$ for $\sigma \to \infty$.

## 5. Case (B): two isoflux and two isothermal walls

In this section, the dimensionless temperature field $t(x,y)$ for the set (B) of thermal boundary conditions is evaluated in order to study the dimensionless velocity field $u(x,y)$ and the friction factor $fRe$ obtained by Eqs. (27) and (28).

In this case, the reference temperature difference is chosen as $\Delta T = aq_w/k$. As a consequence, a positive value of the ratio $Gr/Re$ means either upward mean flow with fluid heating ($q_w > 0$) or downward mean flow with fluid cooling ($q_w < 0$). Obviously, the reverse applies for negative values of the ratio $Gr/Re$. On account of Eqs. (8) and (34), the thermal boundary conditions are expressed in the following dimensionless form

$$\left.\frac{\partial t}{\partial y}\right|_{y=0} = -1, \quad t(0,y) = \eta, \qquad \left.\frac{\partial t}{\partial y}\right|_{y=\sigma} = 1, \quad t(1,y) = \eta. \tag{47}$$

The solution of Eq. (11) with the boundary condition expressed by Eq. (47) is two-dimensional and can be obtained by the use of the finite Fourier transforms. By defining the function $\theta(x,y) = t(x,y) - \eta$ and by considering the finite Fourier sine transform with respect to $x$ [21]

$$\tilde{\theta}(n,y) = \int_0^1 dx\ \theta(x,y)\sin(n\pi x), \tag{48}$$

Eqs. (11) and (47) yield

$$\frac{\partial^2\tilde{\theta}}{\partial y^2} - (n\pi)^2\tilde{\theta} = 0, \qquad \left.\frac{\partial\tilde{\theta}}{\partial y}\right|_{y=0} = -\frac{1-(-1)^n}{n\pi}, \quad \left.\frac{\partial\tilde{\theta}}{\partial y}\right|_{y=\sigma} = \frac{1-(-1)^n}{n\pi}. \tag{49}$$

The solution of Eq. (49) is given by

$$\tilde{\theta}(n,y) = \frac{1-(-1)^n}{(n\pi)^2}\frac{\cosh[n\pi(y-\sigma/2)]}{\sinh(n\pi\sigma/2)}. \tag{50}$$

Therefore, on account of the inversion formula of finite Fourier sine transforms [21], one obtains

$$t(x,y) = \eta + \frac{4}{\pi^2}\sum_{n=1}^{\infty}\frac{\cosh[(2n-1)\pi(y-\sigma/2)]}{(2n-1)^2\sinh[(2n-1)\pi\sigma/2]} \times \sin[(2n-1)\pi x]. \tag{51}$$

As a consequence of Eq. (51), the constraint expressed by Eq. (12) allows one to obtain the following expression of $\eta$:

$$\eta = -\frac{16}{\sigma\pi^4}\sum_{n=1}^{\infty}\frac{1}{(2n-1)^4} = -\frac{1}{6\sigma}, \tag{52}$$

where the identity [24]

$$\sum_{n=1}^{\infty}\frac{1}{(2n-1)^4} = \frac{\pi^4}{96} \tag{53}$$

has been employed.

By employing Eqs. (18), (51) and (52), one readily obtains the double finite Fourier sine transform of $t(x,y)$, namely,

$$\tilde{\tilde{t}}(n,m) = -\frac{1}{\pi^3 n}\left[\frac{\pi}{6m} - \frac{m\sigma\coth(n\pi\sigma/2)}{n(\sigma^2n^2+m^2)}\right] \times [1-(-1)^n][1-(-1)^m]. \tag{54}$$

Substitution of Eq. (54) into Eq. (27) yields

$$u(x,y)=\left[\lambda-\frac{(1+\sigma)^2}{24\sigma^3}\frac{Gr}{Re}\right]\times\left\{\frac{y(\sigma-y)}{2}-\frac{4\sigma^2}{\pi^3}\sum_{n=1}^{\infty}\frac{\cosh[(x-1/2)(2n-1)\pi/\sigma]}{(2n-1)^3\cosh[(2n-1)\pi/(2\sigma)]}\times\sin\left[\frac{(2n-1)\pi y}{\sigma}\right]\right\}+\frac{(1+\sigma)^2}{4\pi^3\sigma}\frac{Gr}{Re}\times\sum_{n=1}^{\infty}\frac{\cosh[(2n-1)\pi(y-\sigma/2)]\sin[(2n-1)\pi x]}{(2n-1)^3\cosh[(2n-1)\pi\sigma/2]}-\frac{(2y-\sigma)(1+\sigma)^2}{4\pi^3\sigma^2}\times\frac{Gr}{Re}\sum_{n=1}^{\infty}\frac{\sinh[(2n-1)\pi(y-\sigma/2)]\sin[(2n-1)\pi x]}{(2n-1)^3\sinh[(2n-1)\pi\sigma/2]},\quad(55)$$

where Eqs. (24) and (25) as well as the Fourier series expansion

$$\frac{\pi^2\tanh[M\pi\sigma/2]}{16M\sigma}\times\left\{\frac{\cosh[M\pi(y-\sigma/2)]}{\cosh[M\pi\sigma/2]}-\frac{2y-\sigma}{\sigma}\frac{\sinh[M\pi(y-\sigma/2)]}{\sinh[M\pi\sigma/2]}\right\}=\sum_{m=1}^{\infty}\frac{(2m-1)\sin[(2m-1)\pi y/\sigma]}{[\sigma^2M^2+(2m-1)^2]^2},\quad(56)$$

in the interval $0\leqslant y\leqslant\sigma$, have been employed.

Eqs. (28), (29) and (54) allow one to evaluate the friction factor $fRe$ as follows:

$$fRe=C_1(\sigma)+C_2(\sigma)\frac{Gr}{Re},\quad(57)$$

where function $C_1(\sigma)$ is defined in Eq. (29) and $C_2(\sigma)$ is given by

$$C_2(\sigma)\equiv C_1(\sigma)(1+\sigma)^2\times\left\{\frac{5\sigma^2-3}{1440\sigma^3}-\frac{2}{3\pi^5}\sum_{n=1}^{\infty}\frac{\tanh[(2n-1)\pi/(2\sigma)]}{(2n-1)^5}+\frac{2}{\pi^5\sigma^2}\sum_{n=1}^{\infty}\frac{1}{(2n-1)^5\sinh[(2n-1)\pi\sigma]}\right\}.\quad(58)$$

Then, the parameter $\lambda$ can be easily evaluated by employing Eqs. (17), (29), (57) and (58). In Table 2, values of $C_2(\sigma)$ are reported.

In Eq. (58), the double infinite sums have been written as single infinite sums by utilizing Eq. (24) integrated in the interval $0\leqslant w\leqslant 1$, Eq. (56) integrated in the interval $0\leqslant y\leqslant\sigma$, Eq. (53) and the identity [24]

$$\sum_{n=1}^{\infty}\frac{1}{(2n-1)^6}=\frac{\pi^6}{960}.\quad(59)$$

An analysis of the velocity profiles given by Eq. (55) allows one to infer that, for any choice of the aspect ratio $\sigma$, there exists an interval $(Gr/Re)_{\mathrm{rev},1}<Gr/Re<(Gr/Re)_{\mathrm{rev},2}$ where no flow reversal occurs. One can prove that the threshold value $(Gr/Re)_{\mathrm{rev},1}$ is negative while $(Gr/Re)_{\mathrm{rev},2}$ is positive and that both these threshold values depend on $\sigma$. For positive values of $Gr/Re$ slightly greater than $(Gr/Re)_{\mathrm{rev},2}$, an onset of flow reversal occurs next to the four corners of the duct. On the other hand, for negative values of $Gr/Re$ slightly smaller than $(Gr/Re)_{\mathrm{rev},1}$, an onset of flow reversal is displayed next to the midpoints of the isoflux boundaries, namely the points $(x=1/2,\ y=0)$ and $(x1/2,\ y=\sigma)$. Indeed, on account of Eqs. (17), (55), (57) and (58), one can prove that $(Gr/Re)_{\mathrm{rev},1}$ and $(Gr/Re)_{\mathrm{rev},2}$ can be expressed as

$$\left(\frac{Gr}{Re}\right)_{\mathrm{rev},1}=\frac{1920\pi^5\sigma^3}{(1+\sigma)^2}\times\left\{\pi^2-8\sum_{n=1}^{\infty}\frac{1}{(2n-1)^2\cosh[(2n-1)\pi/(2\sigma)]}\right\}\times\left(4\left\{\pi^2-8\sum_{n=1}^{\infty}\frac{1}{(2n-1)^2\cosh[(2n-1)\pi/(2\sigma)]}\right\}\times\left\{\pi^5-960\sigma\sum_{n=1}^{\infty}\frac{1}{(2n-1)^5\sinh[(2n-1)\pi\sigma]}\right\}-5\sigma^2\left\{\pi^5-192\sigma\sum_{n=1}^{\infty}\frac{\tanh[(2n-1)\pi/(2\sigma)]}{(2n-1)^5}\right\}\times\left\{\pi^2-32\sigma\sum_{n=1}^{\infty}\frac{(-1)^n}{(2n-1)^2\sinh[(2n-1)\pi\sigma]}\right\}\right)^{-1},\quad(60)$$

$$\left(\frac{Gr}{Re}\right)_{\mathrm{rev},2}=\frac{12\sigma C_1(\sigma)}{1-12\sigma C_2(\sigma)}.\quad(61)$$

Eq. (57) implies that, in the case of purely free convection, i.e., in the limit $\mathrm{d}P/\mathrm{d}Z\to 0$, the mean velocity $U_0$ does not vanish and that its value can be determined through the condition

$$\left.\frac{Gr}{Re}\right|_{\mathrm{d}P/\mathrm{d}Z\to 0}=-\frac{C_1(\sigma)}{C_2(\sigma)}.\quad(62)$$

Moreover, Eqs. (31) and (55) imply that, in the limit $\mathrm{d}P/\mathrm{d}Z\to 0$, the dimensionless velocity $u^*(x,y)$ can be expressed as

$$u^*(x,y)=-\frac{(1+\sigma)^2}{24\sigma^3}\times\left\{\frac{y(\sigma-y)}{2}-\frac{4\sigma^2}{\pi^3}\sum_{n=1}^{\infty}\frac{\cosh[(x-1/2)(2n-1)\pi/\sigma]}{(2n-1)^3\cosh[(2n-1)\pi/(2\sigma)]}\times\sin\left[\frac{(2n-1)\pi y}{\sigma}\right]\right\}+\frac{(1+\sigma)^2}{4\pi^3\sigma}$$

$$\times \sum_{n=1}^{\infty} \frac{\cosh[(2n-1)\pi(y-\sigma/2)]\sin[(2n-1)\pi x]}{(2n-1)^3\cosh[(2n-1)\pi\sigma/2]}$$

$$-\frac{(2y-\sigma)(1+\sigma)^2}{4\pi^3\sigma^2}$$

$$\times \sum_{n=1}^{\infty} \frac{\sinh[(2n-1)\pi(y-\sigma/2)]\sin[(2n-1)\pi x]}{(2n-1)^3\sinh[(2n-1)\pi\sigma/2]}. \quad (63)$$

## 6. Discussion of the results

In this section, some features of the solutions found in the preceding sections for cases (A) and (B) are described.

### 6.1. Case (A)

As a consequence of Eqs. (38) and (44), the values of function $C_1(\sigma)$ reported in Table 2 allow one to evaluate both the friction factor and the threshold value of $Gr/Re$ for the onset of flow reversal. Therefore, these quantities are decreasing functions of $\sigma$ for $\sigma < 1$, reach a minimum for $\sigma = 1$ and increase for $\sigma > 1$. This feature is expected in the case of the friction factor, since this quantity must be invariant under the change $\sigma \to 1/\sigma$. On the other hand, this behaviour is not trivial in the case of $(Gr/Re)_{\mathrm{rev}}$, since this quantity is influenced by the thermal boundary conditions and the change $\sigma \to 1/\sigma$ does not leave invariant the thermal boundary conditions. If one considers upward mean flow ($Gr/Re > 0$), then one concludes that the smallest threshold value of

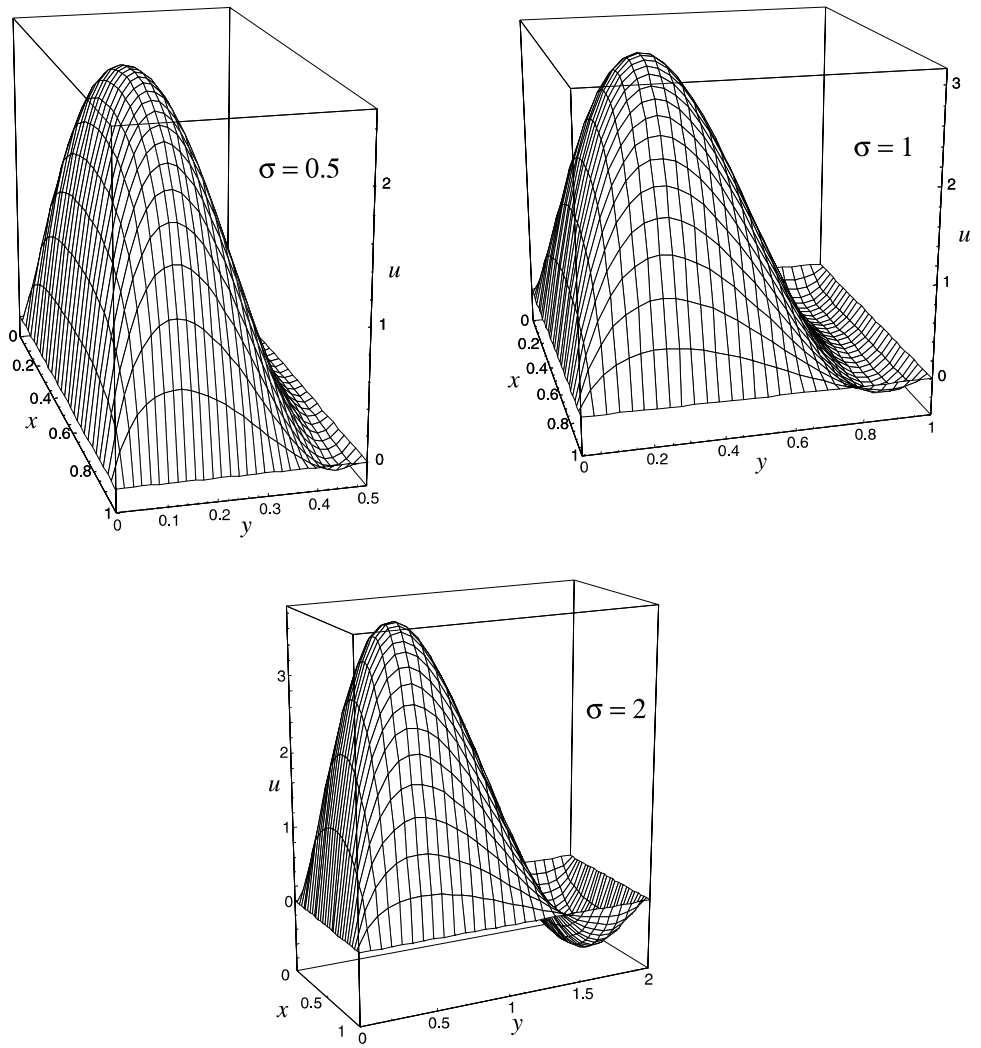


Fig. 3. Set (A) of thermal boundary conditions: plots of $u(x, y)$ for $Gr/Re = 200$.

$Gr/Re$ for the onset of flow reversal occurs when the aspect ratio is 1, i.e., for a square duct. This value is $(Gr/Re)_{rev} = 56.9083$. On account of Table 2 one infers that, in the limit $\sigma \to 0$, $(Gr/Re)_{rev} = 96$. If one employs the polynomial solution which holds in this limit and which is expressed by Eq. (43), one obtains a threshold value for the onset of flow reversal equal to 288. At first sight, these results disagree. However, one should remind that the polynomial solution given by the right-hand side of Eq. (43) holds for a rectangular duct with a very small aspect ratio and far from the shorter boundary walls. On the other hand, the values of $(Gr/Re)_{rev}$ which can be obtained by utilizing Eq. (44) and Table 2 refer to the onset of flow reversal at the corner between two neighbouring walls, i.e. in a region where the polynomial solution expressed by Eq. (43) cannot hold even for extremely small values of $\sigma$.

Fig. 3 refers to $Gr/Re = 200$ and displays the dimensionless velocity distributions with reference to three different aspect ratios: 0.5, 1 and 2. These plots illustrate the effect of flow reversal, which occurs for all the three choices of the aspect ratio. The onset of flow reversal for upward mean flow is shown in Fig. 4 where the aspect ratios 0.5 and 1 are considered. This figure refers to the plane $y = 0.9\sigma$, i.e., a plane parallel to the cool wall and very next to this boundary. Fig. 4 shows that, both for $\sigma = 0.5$ and for $\sigma = 1$, the flow reversal occurs in a region next to the corner between the cool wall and an adiabatic wall and that this region becomes larger as the ratio $Gr/Re$ increases. Fig. 5 displays the behaviour of the distribution $u^*(x,y)$ for purely free convection in the cases $\sigma = 0.5$, $\sigma = 1$ and $\sigma = 2$. These plots reveal an evident antisymmetry with respect to the plane $y = \sigma/2$. Moreover, they show how the average value $\bar{u}^*$ of $u^*(x,y)$ in the region $\{0 < x < 1, 0 < y < \sigma/2\}$ is an increasing function of $\sigma$. Indeed, as it has been pointed out in section 4, $\bar{u}^*$ increases with $\sigma$ for $\sigma < 5.0449$.

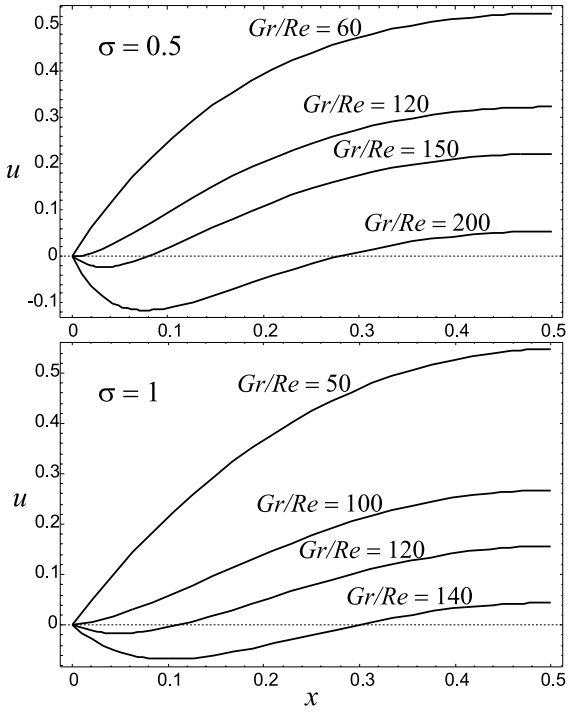


Fig. 4. Set (A) of thermal boundary conditions: plots of $u$ vs $x$ for $y = 0.9\sigma$.

### 6.2. Case (B)

On account of Eq. (57), the quantity $fRe$ for a given pair $(\sigma, Gr/Re)$ can be evaluated by employing the values of $C_1(\sigma)$ and $C_2(\sigma)$ reported in Table 2. One can easily verify that $C_2(\sigma)$ is negative for $\sigma \lesssim 1.1752$, vanishes for $\sigma \simeq 1.1752$ and is positive for $\sigma \gtrsim 1.1752$. Therefore, one can infer that $fRe$ is a linearly decreasing function of $Gr/Re$ for $\sigma \lesssim 1.1752$, is independent of $Gr/Re$ for $\sigma \simeq 1.1752$, is a linearly increasing function of $Gr/Re$ for $\sigma \gtrsim 1.1752$. For instance, if one considers a case of fluid heating ($q_w > 0$) with upward mean flow ($U_0 > 0$), buoyancy reduces $fRe$ when the aspect ratio is lower than about 1.1752, does not affect the value of $fRe$ when the aspect ratio is equal to about 1.1752, increases $fRe$ when the aspect ratio is greater than about 1.1752. Table 1 reveals that the effect of buoyancy on the friction factor is specially strong for very small aspect ratios. It should be pointed out that, for the boundary conditions ($B$), the limit $\sigma \to 0$ is somewhat pathologic. In fact, the isothermal walls become negligibly smaller than the isoflux walls in this limit and, as a consequence, they become inefficient in transferring all the heat supplied by (received from) the isoflux walls, in order to fulfil the requirement $\partial T/\partial Z = 0$. Obviously, the solution found in section 3 holds only if $\partial T/\partial Z = 0$.

Table 2 shows also that a local maximum of $C_2(\sigma)$ occurs in the interval $2.5 < \sigma < 3$. More precisely, one can prove that the local maximum is found for $\sigma \cong 2.6749$. In this table, the values of $-C_1(\sigma)/C_2(\sigma)$ are reported. On account of Eq. (62), these values yield the quantity $Gr/Re$ in the limit $dP/dZ \to 0$, i.e., in the limit of purely free convection. One can easily show that $-C_1(\sigma)/C_2(\sigma)$ is a positive increasing function of $\sigma$ for $\sigma \lesssim 1.1752$, is singular for $\sigma \simeq 1.1752$, it is a negative increasing function of $\sigma$ for $1.1752 \lesssim \sigma \lesssim 2.4161$, it is a negative decreasing function of $\sigma$ for $\sigma \gtrsim 2.4161$. For instance, if one considers a case of fluid heating ($q_w > 0$), purely free convection implies an upward mean flow ($U_0 > 0$) for $\sigma \lesssim 1.1752$, no mean flow ($U_0 = 0$) for $\sigma \simeq 1.1752$, a downward mean flow ($U_0 < 0$) for $\sigma \gtrsim 1.1752$. Distributions of $u^*$ for purely free convection are reported in Fig. 6 with reference to the aspect ratios $\sigma = 0.5$, $\sigma = 1$ and $\sigma = 2$. As is shown in Fig. 6, the qualitative features of the distribution of $u^*$ depend

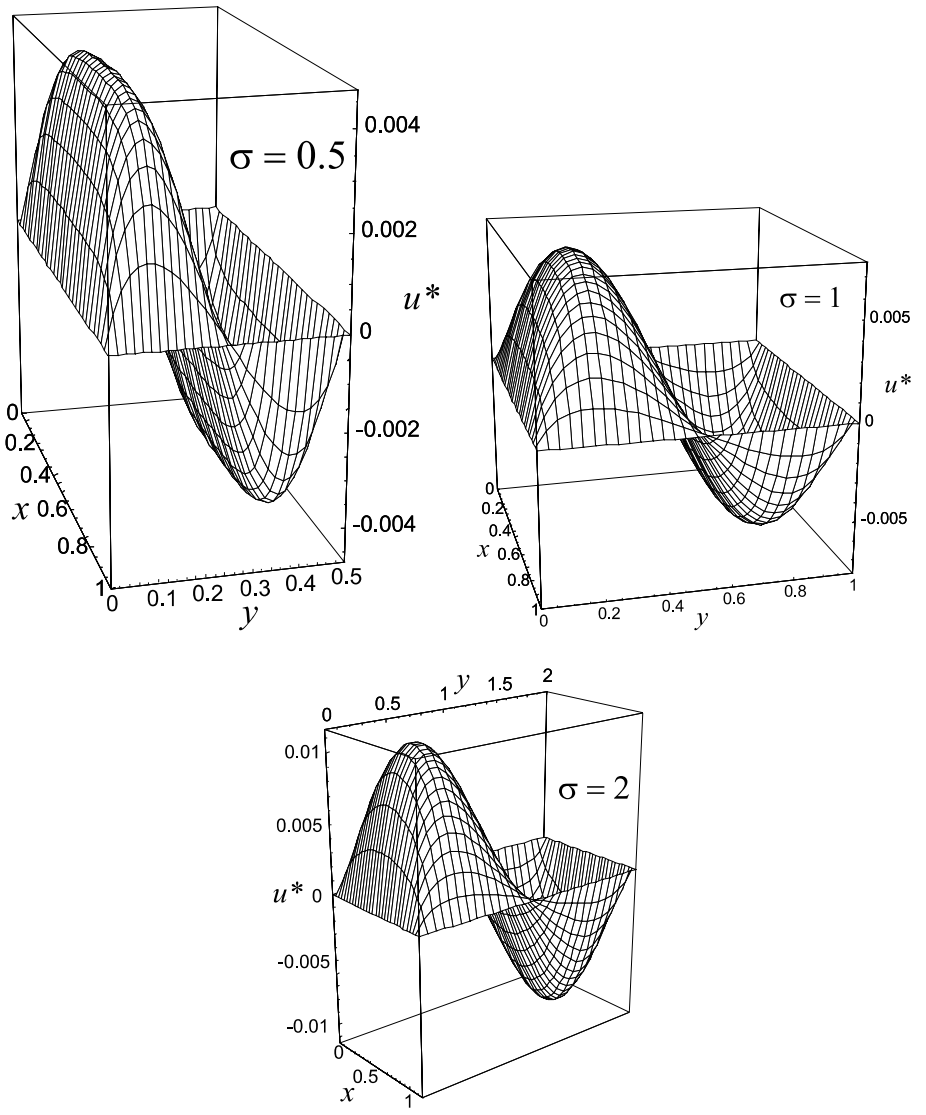


Fig. 5. Set (A) of thermal boundary conditions: plots of $u^*(x,y)$ in the limit $\mathrm{d}P/\mathrm{d}Z \to 0$.

strongly on the aspect ratio. Eqs. (13), (31) and (62) imply that, in the limit $\mathrm{d}P/\mathrm{d}Z \to 0$, the mean value of $u^*$ in a duct cross-section must be equal to $-C_2(\sigma)/C_1(\sigma)$. Indeed, as is easily deduced by employing either Table 2 or Fig. 6, the mean value of $u^*$ is definitely positive for $\sigma = 0.5$ and definitely negative for $\sigma = 2$.

The onset of flow reversal can be predicted by employing the data reported in Table 3. If the heat transfer process is such that $Gr/Re < 0$, i.e., either if $U_0 > 0$ and $q_w < 0$ or if $U_0 < 0$ and $q_w > 0$, the threshold value of $|Gr/Re|$ for the onset of flow reversal depends non-monotonically on the aspect ratio. In particular, $|(Gr/Re)_{\mathrm{rev},1}|$ displays a local maximum for $\sigma \simeq 0.81066$ and a local minimum for $\sigma \simeq 4.7284$. On the other hand, if the heat transfer process is such that $Gr/Re > 0$, the threshold value of $Gr/Re$ for the onset of flow reversal increases monotonically with $\sigma$. Illustrations of the onset of flow reversal are provided in Fig. 7, which refer to a square duct ($\sigma = 1$). Frame (a) of this figure represents the dimensionless velocity distribution at the plane $x = 0.02$ for positive increasing values of $Gr/Re$. The plots show that the flow reversal arises at the corners between an isothermal wall and an isoflux wall. For slightly greater values of $Gr/Re$, an onset of flow reversal occurs also next to the midline of the isothermal walls. The plot for $Gr/Re = 700$ illustrates an instance of flow reversal in a neighbourhood of the whole isothermal wall $x = 0$. Frame (b) of Fig. 7

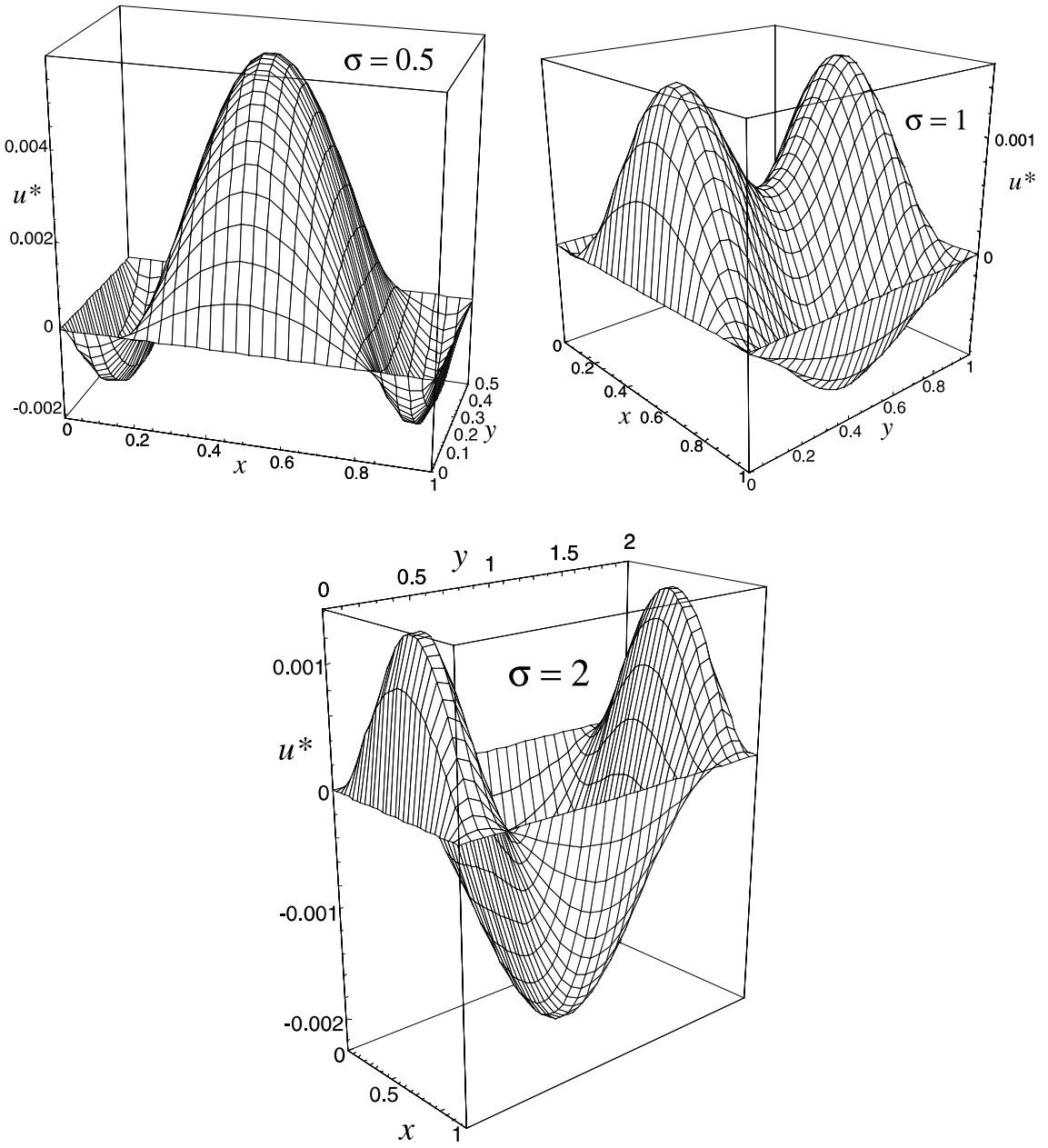


Fig. 6. Set (B) of thermal boundary conditions: plots of $u^*(x,y)$ in the limit $\mathrm{d}P/\mathrm{d}Z \to 0$.

represents the dimensionless velocity distribution at the plane $y = 0.02$ for negative values of $Gr/Re$. In this case, flow reversal arises next to the midline of the isoflux walls.

Finally, in Fig. 8, plots of the dimensionless temperature distribution and of the dimensionless velocity distribution are reported for a square duct. While the dimensionless temperature $t(x,y)$ given by Eq. (51) is independent of $Gr/Re$, the dimensionless velocity $u(x,y)$ depends on $Gr/Re$. In Fig. 8, two plots of $u(x,y)$ have been drawn for $Gr/Re = 1200$ and for $Gr/Re = -1200$, respectively. As one should expect on account of Table 3, the plot of $u(x,y)$ for $Gr/Re = 1200$ displays a flow reversal in the neighbourhood of the isothermal walls. On the other hand, a flow reversal next to the midline of the isoflux walls occurs for $Gr/Re = -1200$.

Table 3
Values of $(Gr/Re)_{rev,1}$ and $(Gr/Re)_{rev,2}$

| $\sigma$ | $-(Gr/Re)_{rev,1}$ | $(Gr/Re)_{rev,2}$ |
|---|---|---|
| 0 | 0 | 0 |
| 0.01 | 5.75486 | 2.82365 |
| 0.05 | 28.7885 | 13.1056 |
| 0.1 | 58.1694 | 24.1172 |
| 0.2 | 122.894 | 42.0469 |
| 0.3 | 200.000 | 56.8869 |
| 0.4 | 284.078 | 70.4316 |
| 0.5 | 361.053 | 83.7783 |
| 0.6 | 418.140 | 97.6193 |
| 0.7 | 450.463 | 112.399 |
| 0.8 | 460.906 | 128.404 |
| 0.9 | 455.994 | 145.818 |
| 1.0 | 442.202 | 164.753 |
| 1.25 | 396.182 | 219.046 |
| 1.5 | 355.431 | 283.139 |
| 1.75 | 325.627 | 356.183 |
| 2 | 304.956 | 436.905 |
| 2.25 | 290.825 | 523.931 |
| 2.5 | 281.190 | 615.996 |
| 2.75 | 274.620 | 712.041 |
| 3 | 270.145 | 811.232 |
| 3.5 | 265.078 | 1016.67 |
| 4 | 262.902 | 1228.91 |
| 4.5 | 262.170 | 1445.98 |
| 5 | 262.179 | 1666.67 |
| 10 | 268.491 | 3966.94 |
| 20 | 275.457 | 8707.48 |
| 100 | 282.948 | 47054.2 |
| $\infty$ | $\infty$ | $\infty$ |

## 7. Conclusions

An analysis of mixed convection in a vertical rectangular duct with, at least, one isothermal wall has been performed with reference to the region of fully developed flow. It has been shown that the dimensionless temperature distribution can be determined independently of the dimensionless velocity field. An analytical solution of the momentum balance equation has been found by employing the method of finite Fourier transforms. This solution yields the dimensionless velocity distribution and the friction factor whenever the dimensionless temperature is known. The following general feature of this solution has been pointed out.

- If the dimensionless temperature distribution $t(x, y)$ is either antisymmetric with respect to the midplane $x = 1/2$ or antisymmetric with respect to the midplane $y = \sigma/2$, then the friction factor is not affected by buoyancy, i.e. the quantity $fRe$ does not depend on the ratio $Gr/Re$.

Two special cases have been investigated: (A) a duct with two facing walls kept isothermal with different temperatures and the others kept insulated; (B) a duct with two facing walls with a uniform wall heat flux and the others kept isothermal with the same temperature.

The main features of the solution in case (A) are the following.

- The friction factor is not influenced by buoyancy, i.e., it does not depend on the ratio $Gr/Re$.
- The onset of flow reversal takes place either at the corners between the cool wall and the adiabatic walls for upward mean flow ($Gr/Re > 0$) or at the corners between the hot wall and the adiabatic walls for downward mean flow ($Gr/Re < 0$).

On the other hand, the behaviour of the solution in case (B) can be described as follows.

- The friction factor is influenced by buoyancy. More precisely, the quantity $fRe$ depends linearly on the ratio $Gr/Re$.
- The onset of flow reversal takes place either at the four corners of the duct in the case $Gr/Re > 0$ or next to the midline of the isoflux walls in the case $Gr/Re < 0$.

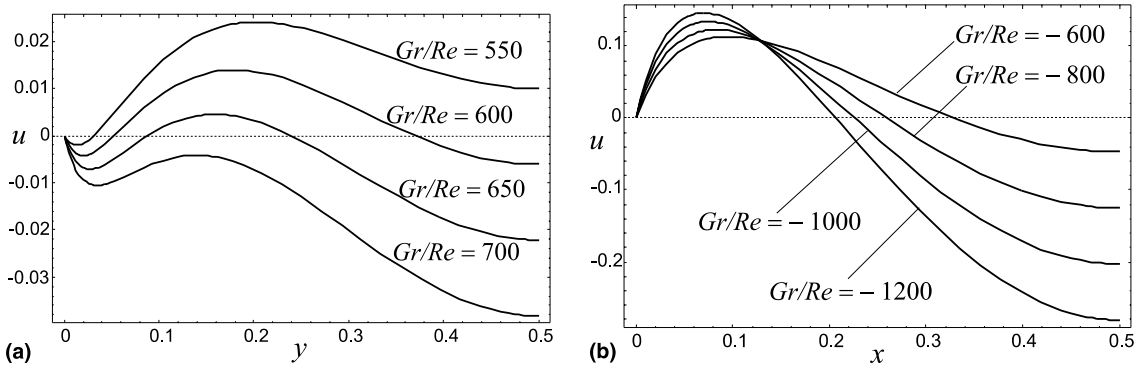


Fig. 7. Set (B) of thermal boundary conditions: (a) plots of $u$ vs $y$ for $\sigma = 1$ and $x = 0.02$; (b) plots of $u$ vs $x$ for $\sigma = 1$ and $y = 0.02$.

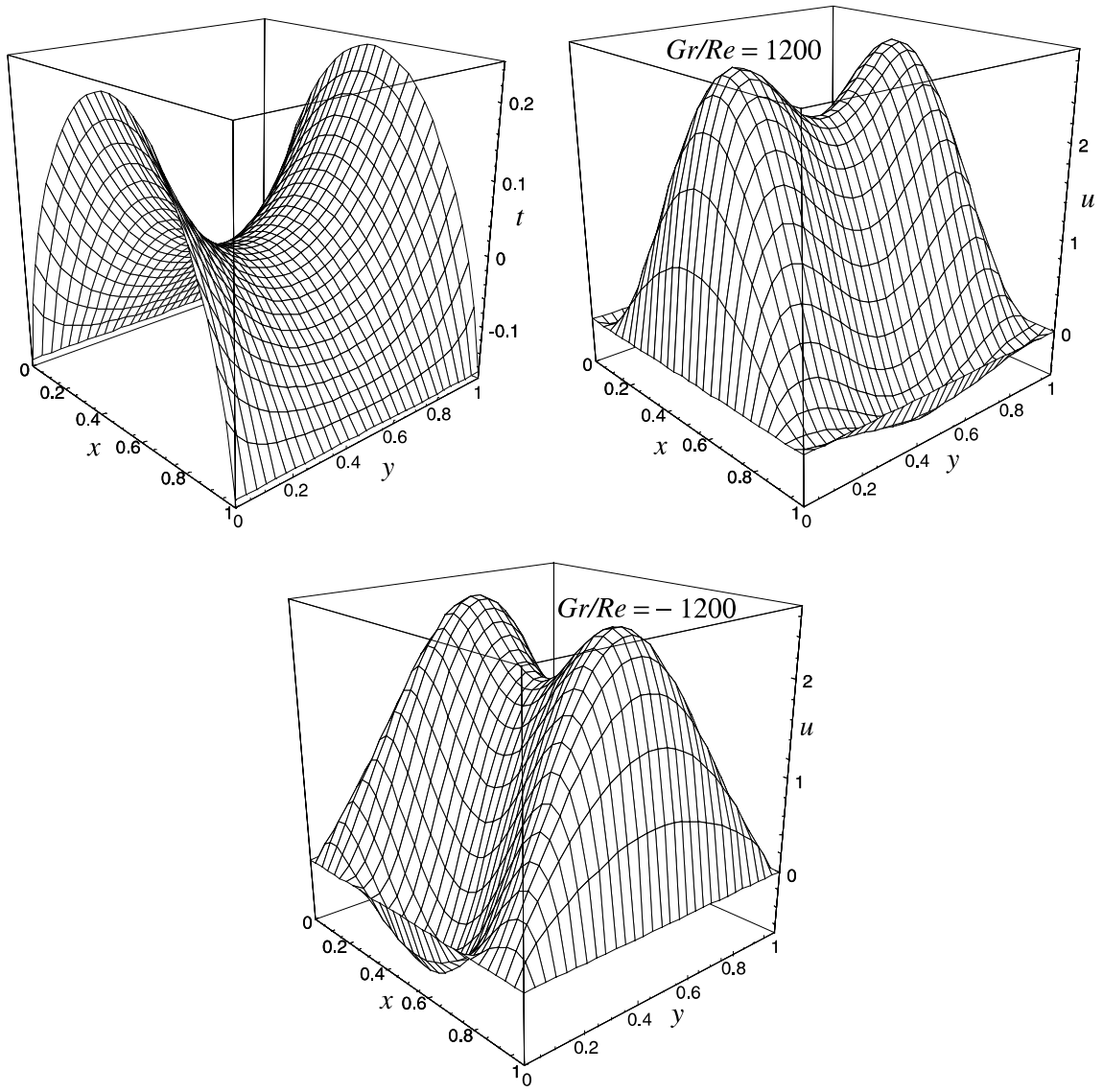


Fig. 8. Set (B) of thermal boundary conditions: plots of $t(x,y)$ and $u(x,y)$ for $\sigma = 1$.

## References

[1] J.P. Hartnett, M. Kostic, Heat transfer to Newtonian and non-Newtonian fluids in rectangular ducts, Adv. Heat Transfer 19 (1989) 247–356.

[2] L.S. Han, Laminar heat transfer in rectangular channels, ASME J. Heat Transfer 81 (1959) 121–128.

[3] M. Iqbal, S.A. Ansari, B.D. Aggarwala, Effect of buoyancy on forced convection in vertical regular polygonal duct, ASME J. Heat Transfer 92 (1970) 237–244.

[4] J.-W. Ou, K.C. Cheng, R.-C. Lin, Combined free and forced laminar convection in inclined rectangular channels, Int. J. Heat Mass Transfer 19 (1976) 277–283.

[5] J.B. Aparecido, R.M. Cotta, Thermally developing laminar flow inside rectangular channels, Int. J. Heat Mass Transfer 33 (1990) 341–347.

[6] C. Nonino, S. Del Giudice, Laminar mixed convection in the entrance region of horizontal rectangular ducts, Int. J. Numer. Meth. Fluids 13 (1991) 33–48.

[7] S.X. Gao, J.P. Hartnett, Non-Newtonian fluid laminar flow and forced convection heat transfer in rectangular ducts, Int. Commun. Heat Mass Transfer 19 (1992) 673–686.

[8] S.X. Gao, J.P. Hartnett, Analytical Nusselt number predictions for slug flow in rectangular duct, Int. Commun. Heat Mass Transfer 20 (1993) 751–760.

[9] B.T.F. Chung, Z.J. Zhang, G. Li, L.T. Yeh, Thermally developing convection from Newtonian flow in rectangular ducts with uniform heating, J. Thermophys. Heat Transfer 7 (1993) 534–536.
[10] M. Spiga, G.L. Morini, The thermal entrance length problem for slug flow in rectangular ducts, ASME J. Heat Transfer 118 (1996) 979–982.
[11] K.-T. Lee, Laminar natural convection heat and mass transfer in vertical rectangular ducts, Int. J. Heat Mass Transfer 42 (1999) 4523–4534.
[12] G.D. McBain, Fully developed laminar buoyant flow in vertical cavities and ducts of bounded section, J. Fluid Mech. 401 (1999) 365–377.
[13] A. Barletta, B. Pulvirenti, Forced convection with slug flow and viscous dissipation in a rectangular duct, Int. J. Heat Mass Transfer 43 (2000) 725–740.
[14] W. Aung, G. Worku, Theory of fully developed, combined convection including flow reversal, ASME J. Heat Transfer 108 (1986) 485–488.
[15] C.-H. Cheng, H.-S. Kou, W.-H. Huang, Flow reversal and heat transfer of fully developed mixed convection in vertical channels, J. Thermophys. Heat Transfer 4 (1990) 375–383.
[16] T.T. Hamadah, R.A. Wirtz, Analysis of laminar fully developed mixed convection in a vertical channel with opposing buoyancy, ASME J. Heat Transfer 113 (1991) 507–510.
[17] A. Barletta, Laminar mixed convection with viscous dissipation in a vertical channel, Int. J. Heat Mass Transfer 41 (1998) 3501–3513.
[18] B.R. Morton, Laminar convection in uniformly heated vertical pipes, J. Fluid Mech. 8 (1960) 227–240.
[19] A. Barletta, Analysis of combined forced and free flow in a vertical channel with viscous dissipation and isothermal-isoflux boundary conditions, ASME J. Heat Transfer 121 (1999) 349–356.
[20] A. Barletta, E. Zanchini, On the choice of the reference temperature for fully-developed mixed convection in a vertical channel, Int. J. Heat Mass Transfer 42 (1999) 3169–3181.
[21] L. Debnath, Integral Transforms and their Applications, CRC Press, New York, 1995 (Chapter 8).
[22] M. Spiga, G.L. Morini, A symmetric solution for velocity profile in laminar flow through rectangular ducts, Int. Commun. Heat Mass Transfer 21 (1994) 469–475.
[23] R.K. Shah, A.L. London, Laminar Flow Forced Convection in Ducts, Academic Press, New York, 1978 (chapter 7).
[24] M.R. Spiegel, in: Mathematical Handbook, McGraw-Hill, New York, 1968.